

Late Ordovician Volcanism of the Northern Part of Altai–Sayan Area and Its Geodynamic Nature

A. A. Vorontsov^{a,b,*}, O. Yu. Perfilova^c, N. N. Kruk^{d,e}, and A. S. Tarasyuk^a

Presented by Academician O.A. Bogatikov January 18, 2017

Received January 18, 2017

Abstract—The results of geological–geochemical studies of some Late Ordovician associations in the frame of the Minusinsk Trough with available geological and U–Pb, Rb–Sr, and K–Ar age dates are presented. The Late Ordovician volcanic rocks form a continuous igneous series, the basalts of which are different from Devonian basalts of the Minusinsk Trough in the lower TiO₂ content (≥ 1.7 wt %) and more fractionated REE pattern. These features should be considered the index characteristics of Late Ordovician rocks. Their compositions reflect processes of fractionation crystallization and mixing of trachibasaltic magmas with crustal melts. When taking into account the regional geological data, it is shown that magmatic activity at the Late Ordovician endogenic evolution stage in the northern part of the Altai–Sayan fold area was caused by the interaction of a mantle plume and the lithospheric mantle, which was metasomatically reworked and enriched in water during former subduction processes.

DOI: 10.1134/S1028334X19040093

During the Early–Middle Paleozoic, the Altai–Sayan fold area (ASFA) was an arena of multiple endogenic events leading to the formation of magmatic halos of various ages. The reasons for this activity are reliably identified for the Cambrian–Early Ordovician with mass formation of anatectic granitic batholiths in collision belts [1–3]. They are also estimated for the Early Devonian characterized by the formation of a system of large juxtaposed troughs and depressions and adjacent large fields of volcanic rocks of higher alkalinity, the formation of which is related to the activity of a mantle plume [4]. There are numerous data indicating that endogenic activity between these events was robust; however, its origin is still unclear. For example, the formation of scattered volcanic and volcanoplutonic halos of moderately alka-

line and alkaline rocks began in the Middle Ordovician far from the margin of the Caledonian continent almost under intraplate conditions [5–7]. During this period, the carbonate-terrigenous shelf sediments indicating the passive margin regime accumulated on the paleocontinent and along its margin [8].

The geodynamic nature of this endogenic activity is a matter of debate, first of all, because of the poor knowledge and the absence of precision geochemical data. In this work, we present the results of petrological–geochemical studies of the Late Ordovician associations with the available geological and U–Pb, Rb–Sr, and K–Ar ages. Our data allowed comparison of the Late Ordovician and Early Devonian volcanic rocks and typical igneous series of various geodynamic settings. This is the background for solution of the problem of the nature of the Late Ordovician endogenic activity in the ASFA.

Late Ordovician volcanism is known in the entire northern part of the ASFA, being most intensive in the frame of the Minusink Trough (Fig. 1) and forming large (> 100 km²) volcanic halos and some paleovolcanoes of the central type (1–20 km²).

The Bolshie Syry volcanic halo is extended along the linear latitudinal zone 10×30 km, which is confined to the southern slope of the Saksyr Ridge in the

^a Vinogradov Institute of Geochemistry, Siberian Branch, Russian Academy of Sciences, Irkutsk, 664033 Russia

^b Irkutsk State University, Irkutsk, 664033 Russia

^c Siberian Federal University, Krasnoyarsk, 660041 Russia

^d Sobolev Institute of Geology and Mineralogy, Siberian Branch, Russian Academy of Sciences, Novosibirsk, 630090 Russia

^e Novosibirsk State University, Novosibirsk, 630090 Russia

*e-mail: voront@igc.irk.ru

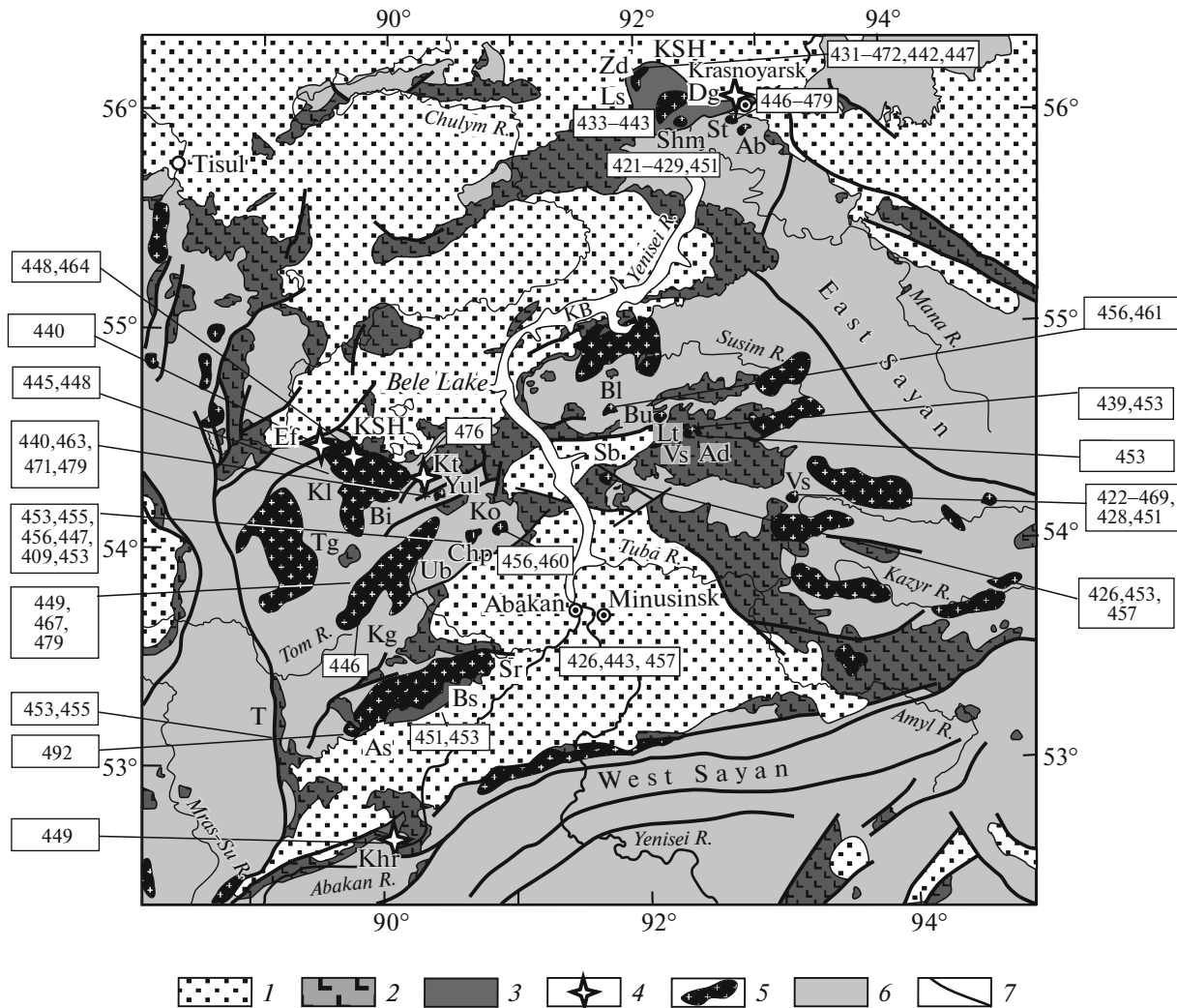


Fig. 1. Location of Late Ordovician igneous associations of the northern part of the Altai-Sayan fold area. 1, Givetian-Carboniferous sedimentary rocks; 2, Early Devonian volcanic halos; 3-5, Late Ordovician volcanic halos: 3, Kacha-Shumikha (KSH), Bolshoi Syr (Bs); 4, paleovolcanoes: Dg, Dolgaya griva; Kt, Katyushkino; Ksh, Koshkulak; Ef, Efremkino; Khr, Kharadzhu; 5, massifs: St, Stolbovskii; Ls, Listvenskii; Shm, Shumikha; Zd, Zeledeevskii; Ab, Abatak; Bl, Bellyk; Bu, Burovskii; Sb, Saibar; Vs, Vysokii; Ib, Irba; Lt, Lutag; Ad, Adrikhinskii; Kl, Kolodzhu; Chp, Chalpan; Ko, Kozhur; Yul, Yula; Bi, Bely Iyus; T, Teya; Kg, Karlygan; batoliths: Sr, Syr; Tg, Tigertysh; As, Askiz; Ub, Uibat; 6, unspecified pre-Late Ordovician geological complexes; 7, faults. KR, Krasnoyarsk reservoir. Rectangles, the K-Ar, Ar-Ar, Rb-Sr, and U-Pb ages (Ma) of igneous complexes are summarized from original data and the data of G.A. Babin, N.N. Kruk, S.N. Rudnev, A.G. Vladimirov, A.E. Izokh, V.V. Vrublevskii, E.I. Berzon, A.G. Rublev, L.P. Rikhvanov, A.N. Smagin, G.A. Ivankin, V.E. Nomokonov, and V.L. Khomichev.

southwestern rim of the Minusinsk Trough. This halo is formed by volcanic, vent, and subvolcanic rocks. The volcanic rocks include intercalating flows of trachybasaltic andesites, trachyandesites, trachytes, trachydacites, and coarse-clastic and lapilli tuffs of intermediate-mafic composition. Their total thickness is >1900 m. The subvolcanic and vent bodies include sills, necks, and dikes of microgabbro, diorites, microsyenites, and microgranites with variable thickness from a few centimeters to 100 m. These rocks are confined to magma-feeding channels, which form a chain oriented in the same direction, as well as the entire magmatic halo. The Rb-Sr age of trachytes

and microsyenites is 451 ± 8 and 453 ± 14 Ma, respectively [7].

The Koshkulak, Efremkino, and Katyushkino paleovolcanoes are located in the western framework of the Minusinsk Trough within the piedmont areas of the Kuznetsk Alatau. The Koshkulak ring paleovolcano with an area of ~ 10 km² is controlled by summits of Bolshoi and Maly Koshkulak mounts, the southwestern slopes of which preserve the fragments of the differentiated volcanic sequence up to ~ 440 m thick overlapping the Late Cambrian rocks with erosion. The basement of the section includes dominant tra-

chybasalts, trachybasaltic andesites, and their tuffs, which upward through the section are replaced by andesites crowned by porphyritic trachytes. The volcanic rocks are intruded by rare bodies of explosive breccias, microsyenites, and porphyry syenites. The hypabyssal syenites and granosyenites are exposed in the northeastern flank of the paleovolcano. The Efremkino paleovolcano is composed of tuffs and lava breccias of trachytes, trachydacites, trachyrhyodacites, and rhyolites, which register the fragments of a poorly preserved vent (1 km²). The Katyushkino paleovolcano of ~17 km² in area is composed of rocks of cover and vent facies, as well as subvolcanic bodies. The volcanic cone is largely eroded: its remnants are preserved as arch ridges a few hundred meters high, where a volcanic sequence (225 m thick in total) is characterized by a flat (5°–10°) periclinal occurrence. The lower part of the section is dominant by trachybasalts and trachybasaltic andesites with trachyandesites and trachydacites upward through the section. The vent part is composed of tuff lavas, explosive breccias, and agglomerate tuffs of mostly trachyte–trachydacites composition. Subvolcanic bodies are rare and include dikes of dolerites and microsyenites composing radial fractures, as well as a bed body of porphyry syenites.

The Dolgaya griva paleovolcano (~10 km²) occurs in the central part of the Kacha–Shumikha depression northeast of the Minusinsk intermontaine trough. The volcano is composed of rocks of volcanic, vent, and subvolcanic facies. The volcanic rocks form a stratified monoclinical (dip NW 30°) sequence up to 2200 m thick with intercalating covers of trachybasalts, trachytes, and tuffs of trachyte–trachyrhyolite–pantellerite composition. The vent facies include a neck of eruptive breccias of trachybasalts and subvolcanic facies are dikes of porphyry trachytes and fine-grained gabbro transiting to trachybasalts in the contact zone, as well as laccoliths of quartz porphyry syenites.

The age of igneous associations of paleovolcanoes is 476–446 Ma (Rb–Sr and K–Ar methods [7] and U–Pb age of zircon [9]).

The composition of rocks and the formation succession of the Late Ordovician and Early Devonian associations [4] are similar, however, they exhibit some specific features. First, the rocks are similar by differentiation with trachybasalts and trachyandesitic basalts in the basements, which are replaced by trachyandesites, trachytes, trachydacites–trachyrhyolites, and rhyolites. The sections rarely contain pantellerites and fragments with irregular intercalation of various rocks. The Late Ordovician associations constantly exhibit vent facies among volcanic rocks, which indicate a wide distribution of paleovolcanoes. The vent facies include pyroclastic and subvolcanic rocks, which form (as well as volcanic rocks) differentiated associations. In contrast, the Early Devonian

sequences show only rare dikes and extrusive bodies of trachytes and dolerite sills.

The contents of major oxides and trace elements of volcanic rocks are shown in Table 1. In the TAS diagram (Fig. 2), the composition points of Late Ordovician volcanic rocks, as well as Early Devonian rocks of the Minusinsk Trough, form a continuous series of mostly moderately alkaline series. Weak distinctions are typical only of the felsic volcanic rocks: the Late Ordovician rhyolitic rocks are more alkaline (the agpaite coefficient reaches 1) in comparison with the Early Devonian. In the Ta–Yb diagram [11] (Fig. 3), the composition points of the Late Ordovician volcanic rocks with the SiO₂ content of 65–76 wt % form a continuous trend from intraplate rocks to volcanic arc granitic rocks.

The multielemental patterns (Fig. 4) of the Late Ordovician volcanic mafic rocks demonstrate enrichment in LILEs and REEs relative to island arc basalts. In contrast to similar Early Devonian basalts of the Minusinsk Trough, they lack TiO₂ (>1.7 wt %) and exhibit a higher degree of REE fractionation, mostly at the expense of the lower contents of Y group elements (HREEs). In the contents of some incompatible elements, they are similar to the OIB composition; however, they are selectively depleted in HFSEs (Nb, Ta, and, to a lesser extent, Zr, Hf, and Ti) and are enriched in Ba and Sr. These features of trachybasalts are inherited by other members of the series: trachybasaltic andesites, trachyandesites, and trachytes (55 wt % < SiO₂ < 64 wt %). At the same time, the contents of incompatible elements in the last group of rocks are systematically lower (Fig. 3) in comparison with their contents of basalts. For example, they have lower Zr, Hf, Nb, Ta, Th, REE, and Y contents, which contradicts the tendency of their accumulation during fractionation, but is explained by mixing of trachybasaltic magmas and their differentiates with crustal anatexic melts depleted in these elements [14]. The felsic (64 wt % < SiO₂ < 76 wt %) volcanic rocks are characterized by higher Rb, Th, U, K, Zr, Hf, and HREE contents (with low Nb and Ta vs. La); lower Ba, Sr, and P contents; and a Eu minimum. This indicates the key role of crystallization differentiation during their formation.

Thus, Late Ordovician volcanic rocks are abundant in the mountainous framework of the Minusinsk Trough and are involved in the structure of both volcanic halos and central-type paleovolcanoes. In spite of the diverse Late Ordovician rock complexes, they form a differentiated compositional association. In contrast to the Early Devonian volcanic rocks of the trough, they are characterized by a lower TiO₂ content (≥1.7 wt % in mafic rocks) and a more fractionated REE pattern of trachybasalts. These features should be ascribed to the index compositional characteristics of the Late Ordovician rocks. Their compositions exhibit two trends of magma evolution. The main process is

Table 1. Compositions of Late Ordovician volcanic rocks

Rock	Bolshie Syry			Koshkulak		Efremkino			Rock	Katyushkino			Dolgaya griva			
	TBA	T	TRD	TBA	TBA	TA	TRD	TR		TB	TB	TB	TB	TBA	T	P
Index	SYR-1/3	SYR-1/6	SYR-1/1	KShk-1/4	KShk-1/2	EFM-1/6	EFM-1/2	EFM-1/7	Index	KTSh-1/8	KTSh-2/3	KTSh-1/4	DGR-1/1	D-68	DRG-1/2	DGR-1/4
SiO ₂	54.19	60.46	67.62	53.91	55.05	58.06	67.58	75.31	SiO ₂	47.75	48.29	49.21	49.18	52.36	66.02	69.13
TiO ₂	0.67	0.55	0.60	1.17	0.94	0.90	0.52	0.22	TiO ₂	1.48	1.12	1.60	1.38	1.55	0.33	0.19
Al ₂ O ₃	18.63	18.88	15.77	16.31	17.37	17.27	15.32	13.09	Al ₂ O ₃	15.04	15.25	15.12	18.42	18.20	15.90	15.07
Fe ₂ O ₃	7.64	5.08	3.11	7.94	5.20	7.46	4.39	1.81	Fe ₂ O ₃	10.51	11.03	10.83	8.45	8.30	5.38	3.29
MnO	0.11	0.04	0.08	0.13	0.14	0.15	0.08	0.03	MnO	0.13	0.15	0.22	0.12	0.09	0.20	0.09
MgO	2.61	1.73	0.74	4.62	3.89	2.79	0.81	0.19	MgO	5.38	5.52	4.85	3.63	3.20	0.09	0.04
CaO	4.85	1.05	0.90	7.97	8.05	5.21	1.76	0.38	CaO	8.98	11.29	9.53	7.85	5.77	0.26	0.44
Na ₂ O	6.23	6.97	5.42	2.58	3.37	4.29	5.30	4.38	Na ₂ O	2.55	3.23	2.52	4.49	4.40	4.98	5.83
K ₂ O	1.39	2.46	4.30	2.47	2.59	1.76	2.60	3.92	K ₂ O	2.80	0.71	1.91	1.63	3.05	5.65	5.07
P ₂ O ₅	0.32	0.53	0.15	0.31	0.48	0.26	0.20	0.04	P ₂ O ₅	0.55	0.35	0.52	0.77	0.99	0.05	0.11
LOI	3.26	2.23	1.19	2.41	2.57	1.78	1.38	0.52	LOI	4.71	3.01	3.57	4.02	1.99	1.11	0.60
Total	99.90	99.97	99.88	99.82	99.65	99.91	99.95	99.88	Total	99.87	99.95	99.87	99.94	99.91	99.96	99.85
A.c.		0.75	0.86				0.75	0.88	A.c.						0.90	1.00
Rb	15	26	89	43	59	24	44	34	Rb	33	18	40	9	48	102	151
Ba	892	674	1193	808	1049	729	687	917	Ba	1694	396	1011	763	839	281	57
Sr	637	319	287	540	1194	584	275	162	Sr	1017	1140	1192	1456	1135	23	7
Zr	111	158	381	265	210	159	242	321	Zr	209	119	234	224	280	631	928
Nb	6	5	15	18	18	7	13	19	Nb	16	9	19	12	14	21	36
Hf	2.8	3.9	9.1	6.4	5.0	3.8	6.0	8.6	Hf	5.2	3.5	5.9	5.3	6.4	13.5	23.0
Ta	0.24	0.32	0.96	1.03	0.99	0.46	0.99	1.30	Ta	0.87	0.50	1.04	0.75	0.74	1.14	2.22

Table 1. (Contd.)

Rock	Bolshie Syry			Koshkulak		Efremkino			Rock	Katyushkino				Dolgaya griva			
	TBA	T	TRD	TBA	TBA	TA	TRD	TR		TB	TB	TB	TB	TB	TBA	T	P
Index	SYR-1/3	SYR-1/6	SYR-1/1	KShK-1/4	KShK-1/2	EFM-1/6	EFM-1/2	EFM-1/7	Index	KTSh-1/8	KTSh-2/3	KTSh-1/4	DGR-1/1	D-68	DRG-1/2	DGR-1/4	
Y	16	16	28	22	16	20	18	30	Y	19	16	22	25	34	45	64	
Th	1.6	3.3	12.1	7.6	6.8	3.9	9.0	12.3	Th	5.9	4.2	6.0	5.8	7.8	12.1	24.0	
U	0.67	0.99	3.90	1.88	1.81	1.35	3.03	3.93	U	1.69	1.17	1.85	1.82	2.73	3.86	8.60	
Pb	17.6	8.2	6.4	13.4	13.0	6.3	10.3	8.6	Pb	14.0	4.7	9.6	11.0	21.0	37.0		
La	22	24	39	35	40	24	28	29	La	41	25	46	52	65	49	69	
Ce	45	52	83	69	81	49	56	66	Ce	87	52	94	118	133	122	162	
Pr	5.8	6.6	9.6	7.8	9.0	5.9	6.8	7.8	Pr	10.4	6.9	11.1	14.0	17.5	14.0	18.0	
Nd	23	26	35	30	35	23	25	28	Nd	43	29	45	55	66	59	70	
Sm	4.5	4.9	7.0	5.7	6.2	4.6	4.5	5.2	Sm	8.0	5.8	8.5	9.2	10.3	11.1	12.7	
Eu	1.54	1.20	1.68	1.48	1.78	1.44	1.33	1.00	Eu	2.19	1.63	2.46	2.25	2.40	1.26	0.64	
Gd	4.2	4.4	6.2	5.5	5.9	4.6	4.2	5.2	Gd	6.8	4.7	7.1	7.3	9.2	10.3	11.3	
Tb	0.65	0.68	1.03	0.78	0.67	0.74	0.72	0.94	Tb	0.88	0.66	1.00	0.91	1.06	1.50	1.84	
Dy	3.40	3.74	5.57	4.56	3.48	4.16	3.74	5.59	Dy	4.39	3.99	5.01	5.08	5.59	9.60	12.10	
Ho	0.74	0.78	1.24	0.89	0.63	0.89	0.83	1.30	Ho	0.79	0.71	0.92	0.98	1.11	1.90	2.54	
Er	1.51	1.70	3.05	2.46	1.67	2.08	1.94	3.32	Er	2.01	1.88	2.34	2.66	3.07	6.10	8.40	
Tm	0.28	0.30	0.54	0.36	0.23	0.37	0.37	0.58	Tm	0.27	0.25	0.32	0.39	0.42	0.88	1.33	
Yb	1.83	1.96	3.59	2.29	1.47	2.31	2.39	3.87	Yb	1.71	1.49	1.98	2.46	2.81	6.60	10.10	
Lu	0.30	0.35	0.61	0.35	0.22	0.38	0.41	0.64	Lu	0.26	0.22	0.30	0.38	0.40	1.07	1.53	

Oxides, wt %; elements, ppm; Fe₂O₃, total iron; A.c., agpaite coefficient. TB, trachybasalts; TBA, trachybasaltic; TA, trachyandesites; T, trachytes, TRD, trachyrhyodacites; P, pannotellurites; TR, trachyrhyolites. The contents of major oxides are determined by X-ray fluorescent analysis at the Vinogradov Institute of Geochemistry, Siberian Branch, Russian Academy of Sciences (IG SB RAS). The content of trace elements was analyzed by ICP MS: at the Center for Collective Use of Isotopic-Geochemical Research of IG SB RAS (open acid decomposition, samples DGR-1/1, D-68, KShK-1/4, KShK-1/2, KTSh-1/8, KTSh-2/3, KTSh-1/4) and the Center for Collective Use, Baikal Center of Nanotechnologies of the Technopark of Irkutsk National Research Technical University (melting with Li metaborate, samples DGR-1/2, DGR-1/4, EFM-1/2, EFM-1/6, EFM-1/7, SYR-1/3, SYR-1/6, SYR-1/1).

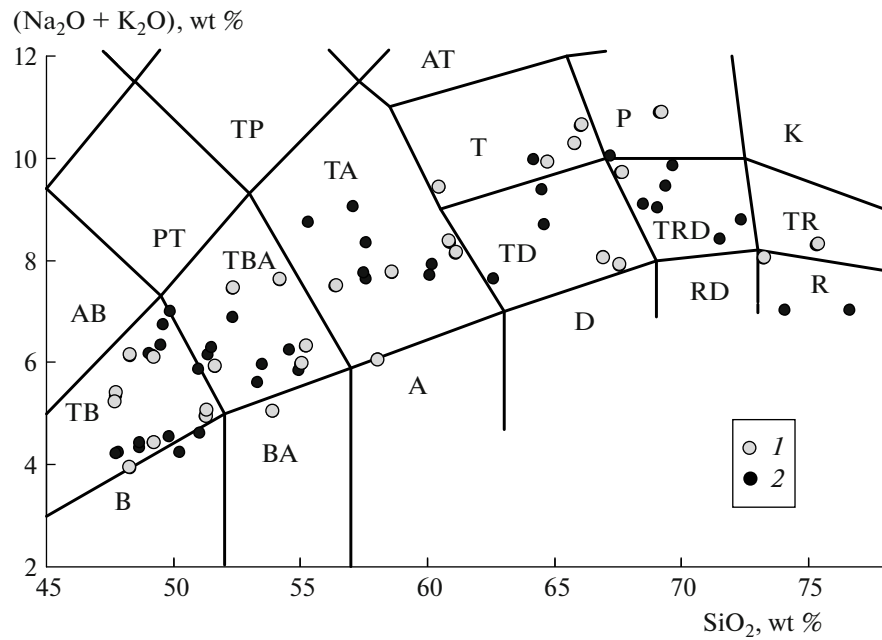


Fig. 2. Classification of Late Ordovician and Early Devonian volcanic associations in the SiO_2 – $(\text{Na}_2\text{O} + \text{K}_2\text{O})$ diagram after [10]. AB, alkali basalts; PT, phonotephrites; TP, tephriphonolites; TB, trachybasalts; B, basalts; BA, basaltic andesites; TBA, trachybasaltic andesites; A, andesites; TA, trachyandesites; D, dacites; TD, trachydacites; T, trachytes, AT, alkali trachytes; RD, rhyodacites; TRD, trachyrhyodacites; P, pantellerites; R, rhyolites; TR, trachyrhyolites; K, komendites. Here and in Fig. 3, Late Ordovician (1) and Early Devonian (2) associations after [4].

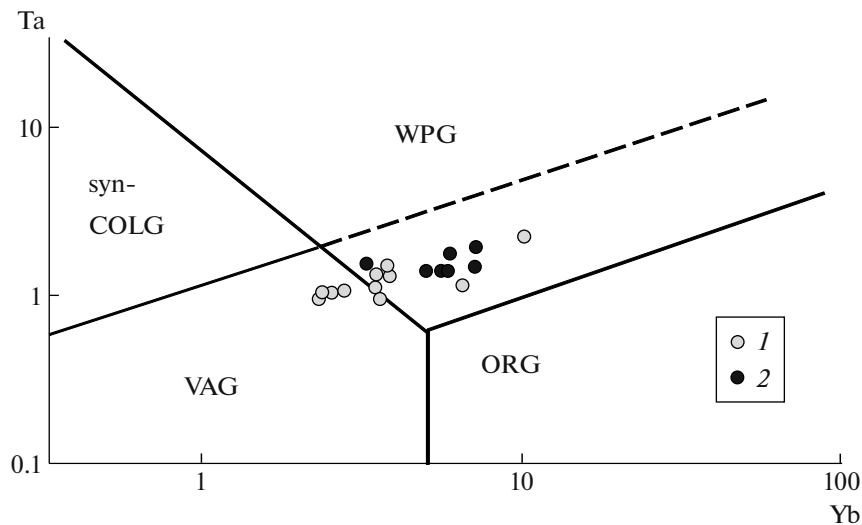


Fig. 3. Compositions of Late Ordovician and Early Devonian volcanic associations with 65–76 wt % SiO_2 in Ta–Yb discriminant diagram of Pearce [11]. Syn-COLG, syncollision granites; VAG, volcanic arc granites; ORG, oceanic ridge granites; WPG, intraplate granites; dotted line, ORG boundary for anomalous ridges.

fractionation crystallization leading to the formation of moderately Ti series of rocks from trachybasalts to trachyrhyolites–rhyolites. Subordinate contamination of melts by crustal material is responsible for the formation of low-Ti trachyandesites with lower contents of incompatible elements including HSE. Both processes reflect the interaction of mantle and crustal

matter sources and occur at active continental margins and areas of intraplate volcanism, which are formed due to the involvement of the mantle plume [15]. In our case, however, the geological data indicate the absence of convergent processes in the region and the intracrustal position of the magmatic area. This geological constraint allows the conclusion that, in

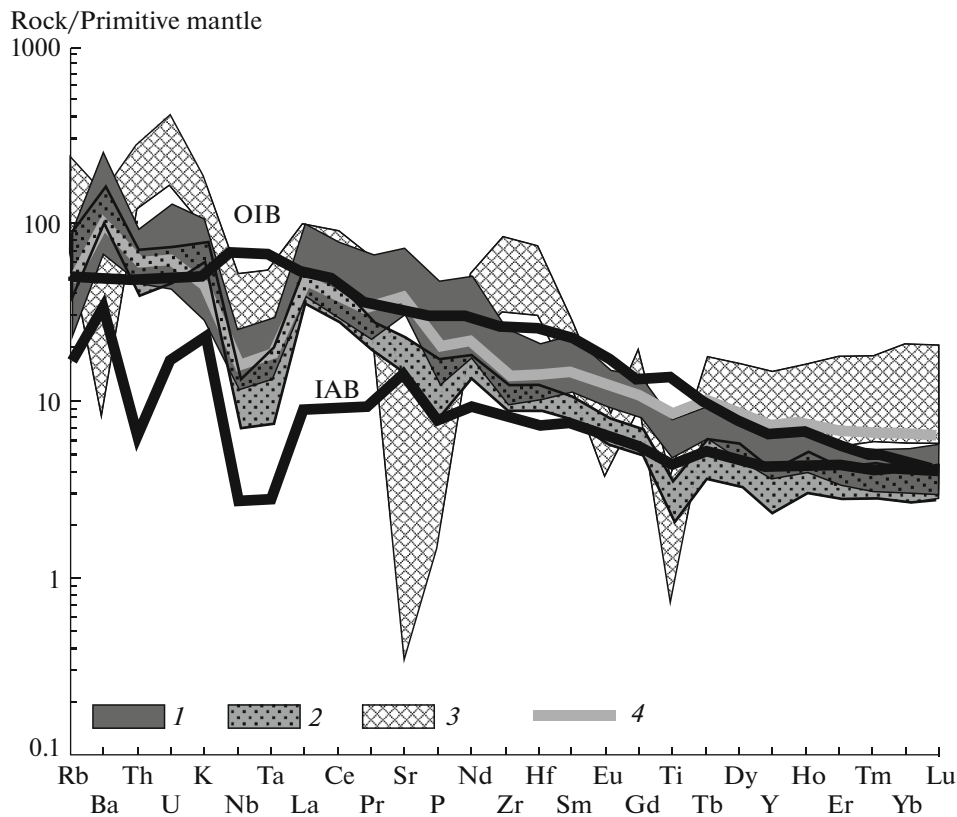


Fig. 4. Spider-diagram for Late Ordovician and Early Devonian volcanic associations. 1–3, Late Ordovician rocks: 1, trachybasalts and trachybasaltic andesites, $48\% < \text{SiO}_2 < 55\%$; 2, trachyandesites and trachytes, $55\% < \text{SiO}_2 < 64\%$; 3, trachydacites, trachyrhyolites, and rhyolites, $64\% < \text{SiO}_2 < 76\%$; 4, mean composition of Early Devonian basalts (Batenevskii uplift [4]). The compositions of primitive mantle and oceanic island basalts (OIB) are after [12]; island arc basalts [13].

spite of lacking mafic rocks with apparent intraplate geochemical features among the igneous rocks, the Late Ordovician magmatism of the northern part of the ASFA was most likely caused by the activity of the mantle plume. This conclusion is in line with the compositional features of igneous rocks: they belong to subalkaline and alkaline petrochemical series and are enriched in most lithophile elements. Similar features of parental magmas are typical of the Central Asian foldbelt, where mantle plumes affect the lithospheric mantle, which was metasomatically reworked during the former Vendian–Cambrian subduction [1, 3] related to the evolution of the Kuznetsk–Alatau and Altai–North Sayan island arc systems.

FUNDING

This work was supported by the Russian Foundation for Basic Research, project no. 16-05-00181, and the Science School Chemical Geodynamics, project no. NSh 9638.2016.5.

REFERENCES

1. M. I. Kuzmin and V. V. Yarmolyuk, *Russ. Geol. Geophys.* **55** (2), 120–143 (2014).
2. A. G. Vladimirov, A. E. Izokh, G. V. Polyakov, G. A. Babin, A. S. Mekhonoshin, N. N. Kruk, V. V. Khlestov, S. V. Khromykh, A. V. Travin, D. S. Yudin, R. A. Shelepaev, I. V. Karmysheva, and E. I. Mikheev, *Petrology* **21** (2), 158–180 (2013).
3. S. N. Rudnev, *Early Paleozoic Granitoid Magmatism of the Altai-Sayan Folded Area and Ozernaya Zone of Western Mongolia* (Siberian Branch Russ. Acad. Sci., Novosibirsk, 2013) [in Russian].
4. A. A. Vorontsov, V. V. Yarmolyuk, G. S. Fedoseev, O. Yu. Perfilova, V. F. Posokhov, A. V. Travin, and T. F. Gazizova, *Petrology* **23** (4), 353–375 (2015).
5. A. E. Izokh, R. A. Shelepaev, A. V. Lavrenchuk, E. V. Borodina, V. V. Egorova, E. A. Vasyukova, and D. P. Gladkochub, in *Proc. Conf. "Geodynamic Evolution of Central Asian Mobile Belt Lithosphere (From the Ocean to Continent)"* (Inst. Earth's Crust Siberian Branch Russ. Acad. Sci., Irkutsk, 2005), Vol. 1, pp. 106–108 [in Russian].
6. A. G. Rublev, Yu. P. Shergina, and E. I. Berzon, *Otech. Geol.*, No. 3, 47–54 (1999).
7. O. Yu. Perfilova, M. L. Makhlaev, and S. D. Sidoras, *Litosfera*, No. 3, 137–152 (2004).
8. N. A. Berzin and L. V. Kungurtsev, *Geol. Geofiz.* **37** (1), 63–81 (1996).

9. N. N. Kruk, G. A. Babin, A. G. Vladimirov, S. N. Rudnev, A. S. Gibsher, Yu. K. Sovetov, S. A. Sergeev, A. B. Kotov, E. B. Sal'nikova, O. A. Levchenko, E. N. Makhlaev, and A. G. Derban, in *Petrology of Magmatic and Metamorphic Complexes* (Tomsk Polytechnic Univ., Tomsk, 2002), Vol. 1, pp. 189–193 [in Russian].
10. *Petrological Code. Magmatic, Metamorphic, Metasomatic, Impact Units* (Karpinsky Russ. Geol. Res. Inst., St. Petersburg, 2009) [in Russian].
11. J. A. Pearce, N. B. W. Harris, and A. G. Tindle, *J. Petrol.* **25**, 956–983 (1984).
12. S. S. Sun and W. F. McDonough, *Geol. Soc. London, Spec. Publ.*, No. 42, 313–345 (1989).
13. T. Churikova, F. Dorendorf, and G. Worner, *J. Petrol.* **42** (8), 1567–1593 (2001).
14. B. A. Litvinovsky, V. V. Yarmolyuk, A. N. Zanvilevich, M. G. Shadaev, A. V. Nikiforov, and V. F. Posokhov, *Geochem. Int.* **43** (12), 1149–1167 (2005).
15. V. V. Yarmolyuk and V. I. Kovalenko, *Petrology* **11** (6), 504–531 (2003).

Translated by I. Melekestseva